IOPscience iopscience.iop.org

Home Search Collections Journals About Contact us My IOPscience

Nitride light-emitting diodes

This article has been downloaded from IOPscience. Please scroll down to see the full text article.

2001 J. Phys.: Condens. Matter 13 7089

(http://iopscience.iop.org/0953-8984/13/32/314)

View the table of contents for this issue, or go to the journal homepage for more

Download details:
IP Address: 171.66.16.226
The article was downloaded on 16/05/2010 at 14:06

Please note that terms and conditions apply.

INSTITUTE OF PHYSICS PUBLISHING JOURNAL OF PHYSICS: CONDENSED MATTER

J. Phys.: Condens. Matter **13** (2001) 7089–7098 PII: S0953-8984(01)25169-8

Nitride light-emitting diodes

T Mukai[1], S Nagahama[1], N Iwasa[2], M Senoh[2] and T Yamada[2]

[1] Nitride Semiconductor Research Laboratory, Nichia Corporation, 491 Oka, Kaminaka, Anan, Tokushima 774-8601, Japan
[2] Department of Research and Development, Nichia Corporation, 491 Oka, Kaminaka, Anan, Tokushima 774-8601, Japan

Received 24 May 2001
Published 26 July 2001
Online at stacks.iop.org/JPhysCM/13/7089

Abstract

We review the progress in the field of InGaN-based light-emitting diodes (LEDs) and discuss the issue of threading dislocations and the luminous efficiency. The first candela-class blue LEDs have been developed. An InGaN layer was used to produce these LEDs instead of a GaN active layer. The quantum-well structure InGaN active layer dramatically improved the external quantum efficiency. There are a number of threading dislocations in nitride-based LEDs. InGaN LEDs, however, have quite high external quantum efficiency. With regard to this, it is thought that the fluctuation of the indium mole fraction is strongly related to the high external quantum efficiency. Considering the density of threading dislocations in the nitride-based LEDs, we discuss what can improve the external quantum efficiency of nitride-based LEDs.

1. Introduction

III–V nitride-based semiconductors have direct band gaps. The band-gap energy of AlGaInN varies between 6.2 and 2.0 eV depending on composition. Therefore, by using these semiconductors, devices emitting over the range from ultraviolet (UV) to red can be fabricated. The non-availability of single-crystalline substrates or other high-quality single-crystalline substrates with the same lattice parameters as GaN made GaN growth difficult. For this reason, sapphire and SiC have been used for the epitaxial growth of nitrides. One of the major breakthroughs in the growth of high-quality nitride films was the development of the low-temperature-grown buffer layer technique [1, 2]. Using sapphire substrates, thin AlN or GaN buffer layers grown at low temperature improved the quality of the GaN film grown at high temperature remarkably. The achievement of p doping using Mg and its activation treatment constituted one of the key breakthroughs in the development of GaN technology. Low-energy electron-beam-irradiated Mg-doped GaN exhibited lower resistivity and the PL intensity dramatically improved [3]. Also Nakamura *et al* achieved even higher p doping and uniform activation of Mg by using thermal annealing under a N_2 ambient [4]. Highly efficient InGaN light-emitting diodes (LEDs) have been developed on the basis of these breakthroughs

 © 2001 IOP Publishing Ltd Printed in the UK

[1–4]. Each of these light-emitting devices uses an InGaN active layer instead of a GaN active layer, because it is difficult to fabricate highly efficient LEDs using a GaN active layer. The InGaN active layer in these LEDs includes a large number of threading dislocations, from 1×10^8 to 1×10^{12} cm^{-2}, originating from the interface between the GaN and sapphire substrate due to the large lattice mismatch of 15% [5, 6]. In spite of this large number of dislocations, the efficiency of the InGaN-based LEDs and laser diodes (LDs) is high, as is that of the conventional III–V compound semiconductor-based LEDs and LDs. The density of both point defects and structural defects in the materials has limited the device performance of the conventional optoelectronic device. However, III–V nitride-based LEDs are less sensitive to dislocations than conventional III–V semiconductors. Epitaxially laterally overgrown GaN (ELOG) was developed recently; this has a reduced number of threading dislocations in the GaN epitaxial layers [7–9]. Using ELOG, the number of threading dislocations was reduced significantly in the GaN grown on a SiO_2 stripe. The characteristics of nitride-based LEDs grown on both ELOG and sapphire substrates are described. The performances of the latest InGaN-based LEDs are also described in this paper.

2. The first candela-class blue LEDs

The first candela-class blue LEDs were fabricated using a Zn-doped InGaN active layer. Because a higher In content in the InGaN layer causes a decrease of the luminescence intensity, InGaN with a relatively low In content was used. To obtain blue emission, Zn-doped InGaN layers were used as the active layer. Figure 1 shows the cross section of the InGaN/AlGaN double-heterostructure (DH) LEDs. InGaN films were grown by the two-flow metallo-organic chemical vapour deposition (MOCVD) method. Details of two-flow MOCVD are described in other articles [10, 11]. The growth was conducted at atmospheric pressure. Two-inch-diameter sapphire with (0001) orientation (*c*-face) was used as the substrate. Trimethylgallium (TMG), trimethylaluminium (TMA), trimethylindium (TMI), monosilane (SiH_4), bis-cyclopentadienylmagnesium (Cp_2Mg), diethylzinc (DEZ) and ammonia (NH_3)

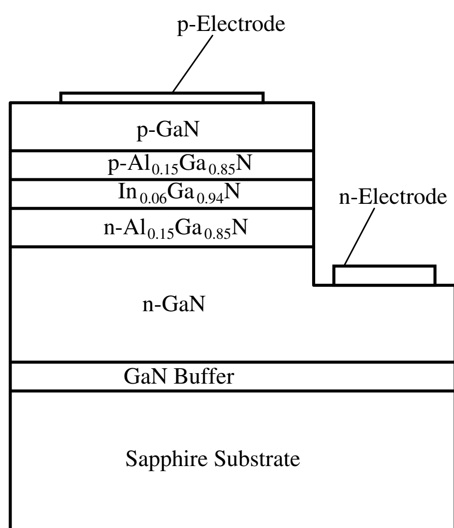

Figure 1. The structure of the InGaN/AlGaN double-heterostructure LEDs.

were used as Ga, Al, In, Si, Mg and N sources, respectively. First, the substrate was heated to 1050 °C in a stream of H_2. Then, the substrate temperature was lowered to 510 °C to grow the GaN buffer layer. The thickness of the GaN buffer layer was about 300 Å. Next, the substrate temperature was elevated to 1020 °C to grow the GaN films. During the deposition, the flow rates of NH_3, TMG and SiH_4 (10 ppm Si in H_2) in the main flow were maintained at 4.0 l min^{-1}, 30 μmol min^{-1} and 4 nmol min^{-1}, respectively. The flow rates of H_2 and N_2 in the subflow were both maintained at 10 l min^{-1}. The Si-doped GaN films were grown for 60 min. The thickness of the Si-doped GaN film was approximately 4 μm. After GaN growth, a Si-doped $Al_{0.15}Ga_{0.85}N$ layer was grown to a thickness of 0.15 μm by feeding in TMA and TMG. After the Si-doped $Al_{0.15}Ga_{0.85}N$ growth, the temperature was decreased to 800 °C and a Zn-doped $In_{0.06}Ga_{0.94}N$ layer was grown for 15 min. During the $In_{0.06}Ga_{0.94}N$ growth, the flow rates of TMI, TEG and NH_3 in the main flow were maintained at 17 μmol min^{-1}, 1.0 μmol min^{-1} and 4.0 l min^{-1}, respectively. The Zn-doped InGaN films were grown by introducing DEZ at the flow rate of 10 nmol min^{-1}. The thickness of the Zn-doped InGaN layer was about 500 Å. After the Zn-doped InGaN growth, the temperature was increased to 1020 °C to grow Mg-doped p-type $Al_{0.15}Ga_{0.85}N$ and GaN layers by passing TMA, TMG and Cp_2Mg through. The thicknesses of the Mg-doped p-type $Al_{0.15}Ga_{0.85}N$ and GaN layers were of 0.15 μm and 0.5 μm, respectively. A p-type GaN layer was grown as the contact layer of a p-type electrode in order to improve the ohmic contact. After the growth, N_2 ambient thermal annealing was performed to obtain a highly p-type GaN layer at a temperature of 700 °C [4]. Fabrication of LED chips was accomplished as follows. The surface of a p-type GaN layer was partially etched until the n-type GaN was exposed. Next, a Ni/Au contact was evaporated onto the p-type GaN layer and a Ti/Al contact onto the n-type GaN layer. The wafer was cut into a rectangular shape. These chips were set on the lead frame and were then moulded. The characteristics of the LEDs were measured under direct-current-biased conditions at room temperature (RT). The peak wavelength is 450 nm and the full width at half-maximum (FWHM) of the peak emission is 70 nm for a forward current of 10 to 40 mA. The output power and the external quantum efficiency at 20 mA are 1500 μW and 2.7%, respectively.

3. Quantum-well structure InGaN LEDs

In order to obtain blue and blue–green emission centres in InGaN/AlGaN DH LEDs, Zn doping of the InGaN active layer was performed. The longest peak wavelength of the electroluminescence (EL) of InGaN/AlGaN DH LEDs achieved is 500 nm, because the crystal quality of the InGaN active layer of DH LEDs becomes poor when the indium mole fraction is increased to obtain a green band-edge emission. When the InGaN active layer becomes thin, the elastic strain is not relieved by the formation of misfit dislocations and the crystal quality of the InGaN active layer improves. Quantum-well (QW) structure LEDs [12, 13] that have a thin InGaN active layer are described in this section. Figure 2 shows the green LED device QW structure. The green LED device structures consist of a GaN buffer layer 300 Å thick grown at low temperature (550 °C), a layer of n-type GaN:Si 4 μm thick, an active layer of undoped $In_{0.45}Ga_{0.55}N$ 30 Å thick, a layer of p-type $Al_{0.2}Ga_{0.8}N$:Mg 1000 Å thick, and a layer of p-type GaN:Mg 0.5 μm thick. The active region forms a single-quantum-well (SQW) structure consisting of a $In_{0.45}Ga_{0.55}N$ well layer 30 Å thick sandwiched by barrier layers of n-type GaN, 4 μm thick, and p-type $Al_{0.2}Ga_{0.8}N$, 1000 Å thick. The output power of the SQW LEDs is shown as a function of the forward current in figure 3. The output power of the blue and green SQW LEDs increases sublinearly up to 40 mA as a function of the forward current. Above 60 mA, the output power almost saturates. The reason for this will be discussed in section 5. At the forward current of 20 mA, the output power and the external quantum efficiency of blue

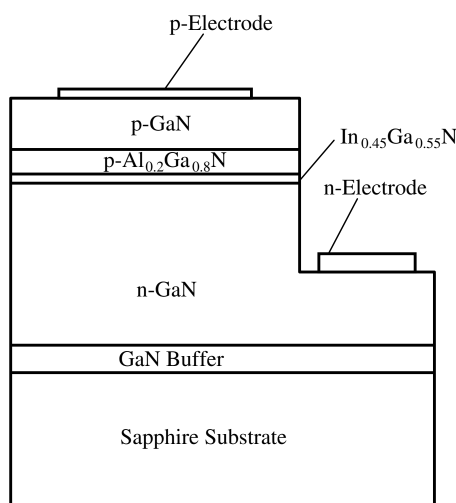

Figure 2. The structure of green SQW LEDs.

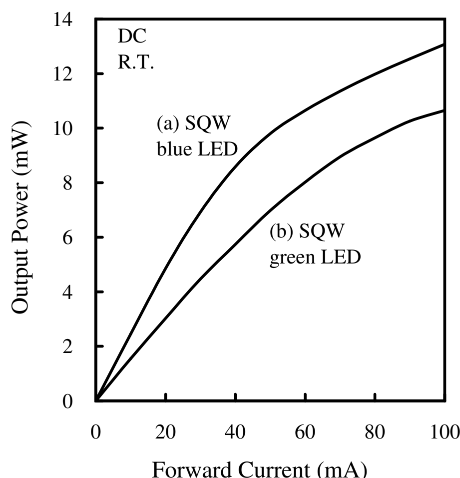

Figure 3. The output power of (a) blue and (b) green SQW LEDs as functions of the forward current.

SQW LEDs are 5 mW and 9.1%, respectively. Those of the green SQW LEDs are 3 mW and 6.3%, respectively. The output power of green LEDs is relatively low in comparison with that of blue SQW LEDs, probably due to the poor crystal quality of the InGaN well layer which has large lattice mismatch and difference in thermal expansion coefficients between the well and barrier layers. The peak wavelength and the FWHM of the typical blue SQW LEDs are 450 nm and 20 nm, respectively, and those of green SQW LEDs are 520 nm and 30 nm, respectively. Also, blue and green LEDs that have multi-quantum-well (MQW) structure active layers were fabricated. The device structure of MQW LEDs is almost the same as that of SQW LEDs, except for the active layer. The MQW structure active layer for a blue LED consists of six undoped $In_{0.27}Ga_{0.73}N$ well layers 30 Å thick sandwiched by seven GaN barrier layers 150 Å thick. At the forward current of 20 mA, the output power and the external quantum efficiency of blue MQW LEDs are 11 mW and 20.6%, respectively. Those of the green MQW LEDs are 8 mW and 16.8%, respectively.

4. Amber and UV InGaN LEDs

In this section, amber InGaN LEDs [14] and UV InGaN LEDs [15] are described. The amber InGaN LED device structure consists of a GaN buffer layer 300 Å thick grown at low temperature (550 °C), a layer of undoped GaN 0.7 μm thick, a layer of n-type GaN:Si 3.3 μm thick, a layer of undoped GaN (the current-spreading layer) 400 Å thick, an active layer of undoped InGaN 25 Å thick, a layer of p-type $Al_{0.2}Ga_{0.8}N$:Mg 300 Å thick and a layer of p-type GaN:Mg 0.2 μm thick. It was difficult to determine the exact indium composition of the InGaN active layer due to the weak signal intensity in x-ray diffraction and photoluminescence measurements. Unlike the above-mentioned InGaN-based LEDs (sections 2 and 3), the n-type GaN:Si was replaced by undoped GaN and n-GaN:Si. The undoped GaN layer with a high resistivity between the InGaN active and n-GaN layers was used to uniformly spread a current over the InGaN active layer. Fabrication of LED chips was accomplished in the above-described way. The characteristics of the LEDs were measured under direct-current-

biased conditions at RT, except for the measurement of the temperature dependence of the output power. The typical forward voltage was 3.3 V at a forward current of 20 mA. The peak wavelength and the FWHM of the emission spectra of the amber InGaN LEDs were 594 nm and 50 nm, respectively. Figure 4 shows the output power of amber InGaN and AlInGaP LEDs (type: HLMP-DL32, Hewlett-Packard) as a function of the ambient temperature from −30 °C to +80 °C. The output powers of amber InGaN and AlInGaP LEDs at 25 °C were 1.4 mW and 0.66 mW, respectively. The output power of InGaN LEDs was about twice as high as that of AlInGaP LEDs. The output power of each LED was normalized to 1.0 at 25 °C. When the ambient temperature was increased from RT to 80 °C, the output power of amber AlInGaP LEDs decreased dramatically to half that at RT due to a carrier overflow caused by a small band offset between the active layer and cladding layers [16]. In the AlInGaP system, the band offset is small under conditions of lattice matching of the AlInGaP epilayer and GaAs substrate [16].

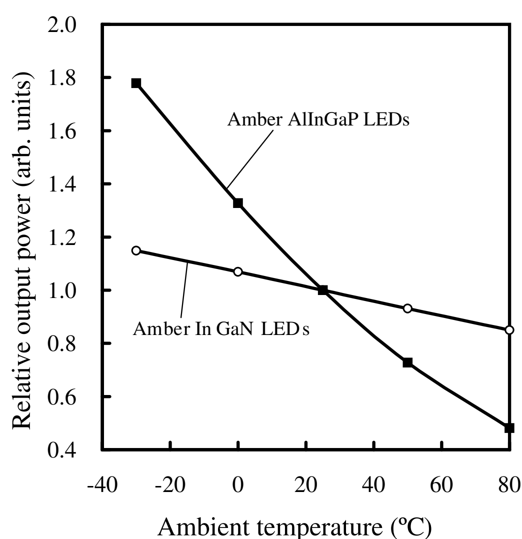

Figure 4. The output power of amber InGaN and AlInGaP LEDs as functions of the ambient temperature from −30 °C to +80 °C. The output power of each LED was normalized to 1.0 at 25 °C.

On the other hand, the temperature dependence of amber InGaN LEDs is relatively weak. When the ambient temperature is increased from RT to 80 °C, the output power of amber InGaN LEDs only decreases to 90% of that at RT, probably due to a small carrier overflow caused by a large band offset between the active layer and cladding layers. In terms of the temperature dependence of the LEDs, InGaN LEDs are superior to the AlInGaP LEDs. On the other hand, the practical GaN-based LEDs with the shortest emission wavelength are UV InGaN LEDs [15]. The UV InGaN LED device structures were almost identical to those of the above-mentioned LEDs except for the InGaN well layer. The indium composition of the InGaN well layer is nearly zero for UV LEDs. InGaN LEDs exhibit peculiar electroluminescence (EL). Figure 5 shows the EL of green InGaN LEDs. Figure 5(a) shows the operating current dependence of the EL. The blue-shift is observed with increasing current due to a band-filling effect of the localized energy states caused by indium composition fluctuation in the InGaN well layer. Figure 5(b) shows the ambient temperature dependence of the EL. There is no change of the EL on changing the ambient temperature. This is a peculiar result because the band-gap

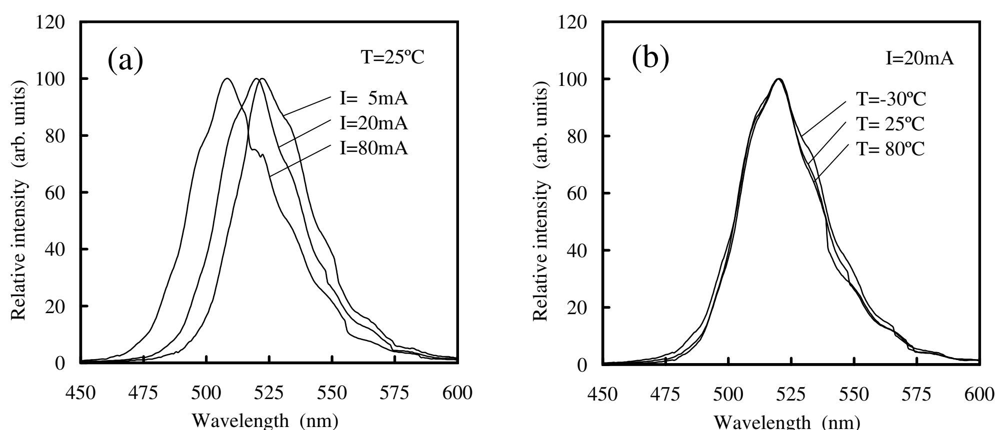

Figure 5. The operating current (a) and ambient temperature (b) dependences of the EL of InGaN green SQW structure LEDs.

energy of semiconductor materials should become smaller with increasing temperature. Thus, the emission peak wavelength should become longer with increasing temperature. The blue InGaN LEDs with an emission peak wavelength of 475 nm showed the same change of the EL as did green LEDs. A blue-shift of the emission peak wavelength with increasing current and no change of the EL with increasing temperature were observed. Figure 6 shows results for the conventional AlInGaP red MQW LEDs (Toshiba TLRH 157P). With increasing temperature, a red-shift of the emission peak wavelength is observed due to the temperature dependence of the band-gap energy, as shown in figure 6(b). On the other hand, there is no change of the emission peak wavelength with increasing operating current due to the lack of localized energy states, as shown in figure 6(a). In view of these results, the band-gap energy of InGaN seems to be independent of temperature. In order to investigate these results further, we studied UV LEDs. Figure 7 shows the EL of UV LEDs with an emission peak wavelength of 380 nm at a current of 20 mA. A small blue-shift of the emission peak wavelength with increasing current is observed due to the small localization energy of the carriers caused by a small In composition

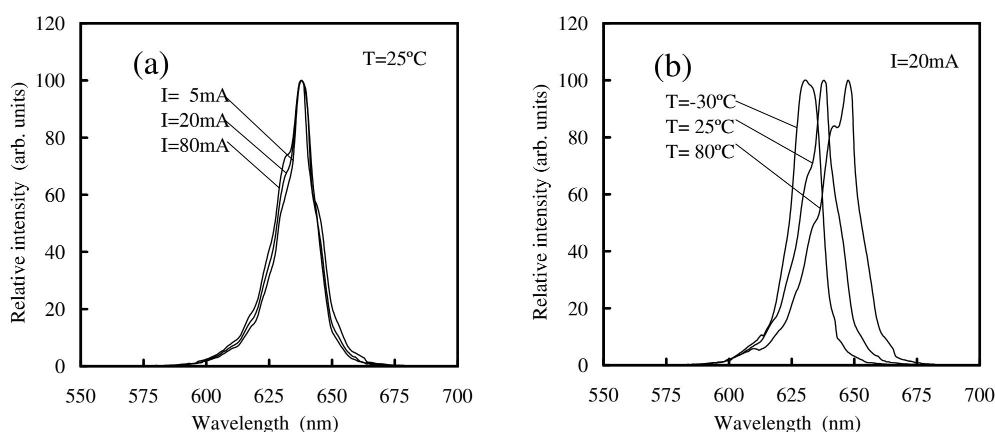

Figure 6. The operating current (a) and ambient temperature (b) dependences of the EL of conventional AlInGaP red LEDs (Toshiba TLRH 157P).

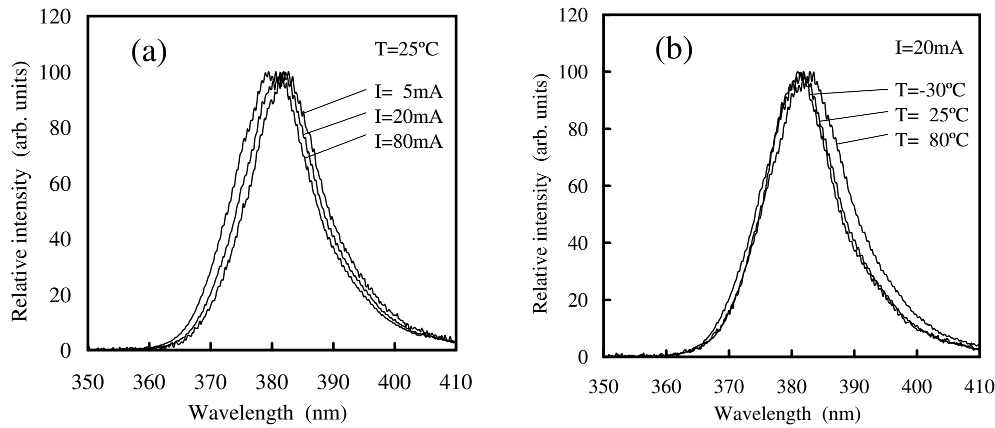

Figure 7. The operating current (a) and ambient temperature (b) dependences of the EL of InGaN UV SQW structure LEDs with an emission peak wavelength of 380 nm.

fluctuation in the InGaN well layer, as shown in figure 7(a). In figure 7(b), almost no change of the emission peak wavelength is observed, as in the case of the green and blue LEDs. Figure 8 shows the EL of UV LEDs with an emission peak wavelength of 375 nm. At this emission peak wavelength, the EL showed a marked change. The emission peak wavelength did not show any change with increasing current, as shown in figure 8(a). On the other hand, a red-shift of the emission peak wavelength was observed with increasing temperature. These emission peak wavelength changes are almost the same as those of conventional AlInGaP LEDs, as shown in figure 6. When we measured the EL of UV LEDs with an emission peak wavelength of 370 nm and a small amount of In (nearly zero), the change of the EL with current and temperature was almost the same as that in figure 8. Thus, there is an abrupt change in the EL at the emission peak wavelength of 375 nm. In other words, there is a change of the emission mechanism at the emission peak wavelength of 375 nm. The UV LEDs with an emission peak wavelength of 375 nm have small localized energy states resulting from small fluctuations in In composition. This means that the emission mechanism is dominated by a conventional

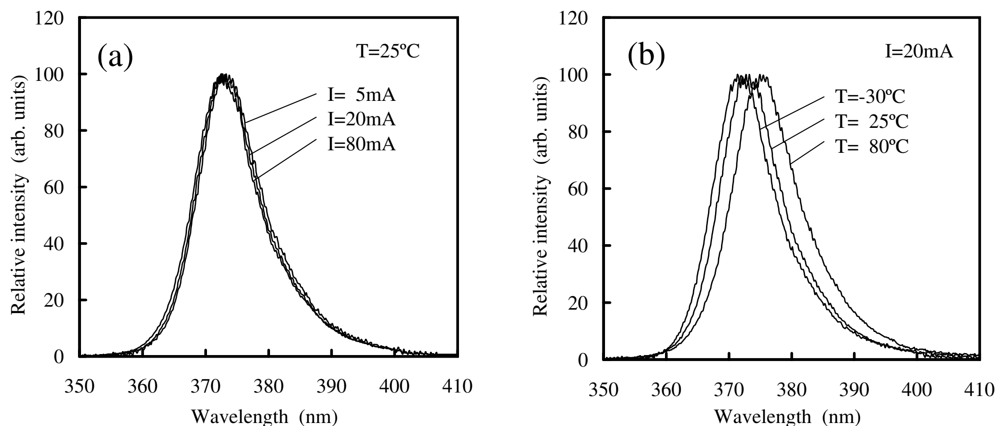

Figure 8. The operating current (a) and ambient temperature (b) dependences of the EL of InGaN UV SQW structure LEDs with an emission peak wavelength of 375 nm.

band-to-band emission, as in AlInGaP LEDs. However, the results in figures 5 and 8 for green/blue/UV LEDs cannot be explained by the simple band-to-band emission mechanism. The large localized energy states due to the large In composition fluctuation seem to be a key factor in the blue-shift with increasing forward current.

However, the constancy of the emission peak wavelength with increasing temperature cannot be explained by just the localized energy states. An additional mechanism is required to explain this constancy of the emission peak wavelength with increasing temperature. When the temperature is increased, the energy distribution of carriers in the localized energy states moves to higher energy levels due to a small density of states. These high-energy carriers may compensate the red-shift of the emission peak wavelength due to the band-gap narrowing caused by increasing temperature.

5. The role of threading dislocations in GaN-based LEDs

Figure 9 shows the relative output power of UV (380 nm) InGaN and GaN LEDs produced using sapphire and ELOG substrates as functions of forward current. The ELOG and GaN on sapphire had average dislocation densities of 7×10^6 cm^{-2} and 1×10^{10} cm^{-1}, respectively. Here, the average dislocation density of the ELOG on sapphire was obtained by dividing the dislocation density of 2×10^7 cm^{-2} on the window region by the ratio (stripe periodicity of 12 μm)/(window width of 4 μm) because the dislocation density on the SiO_2 stripe region was almost zero. The LED chip size is as large as 350 μm $\times$ 350 μm. Each LED chip includes many window and SiO_2 stripe regions. Therefore, we used an average dislocation density for the ELOG on sapphire. The UV GaN LED on ELOG has a much higher (about twofold) output power than that on sapphire. This is because the number of dislocation densities of a GaN LED on ELOG is much smaller than that on sapphire. However, a 380 nm UV InGaN LED on ELOG showed a small increase in output power (25%) in comparison with that on sapphire at 20 mA.

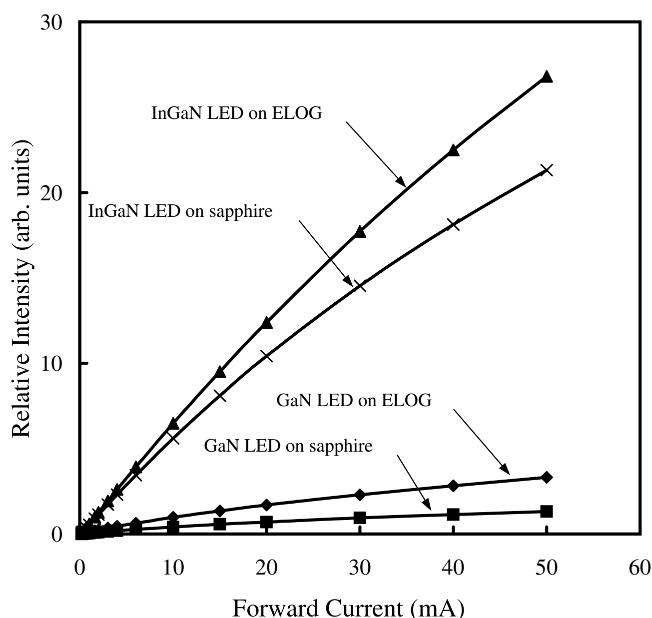

Figure 9. Relative output power of UV InGaN and GaN LEDs as functions of forward current.

This is related to the localized energy state formed by alloy composition fluctuation. When electrons and holes are injected into the GaN active layer of the UV GaN LED on sapphire, they are captured by non-radiative recombination centres formed by a large number of dislocations. Thus, the output power of a UV GaN LED on sapphire is very low. When the dislocation density is reduced by using ELOG, the output power of a UV GaN LED on sapphire can be increased dramatically to twice its initial value. On the other hand, when electrons and holes are injected into the InGaN active layer of a UV InGaN LED on sapphire, the carriers are easily captured by deep localized states formed by alloy composition fluctuations, and then recombine radiatively before they are captured by non-radiative recombination centres formed by a large number of dislocations [17, 18]. However, when the depth of the localized energy states is small, such as in UV InGaN LEDs due to a small In mole fraction in the InGaN well layer, some carriers overflow from the localized energy states with increasing current and reach non-radiative recombination centres formed by a large number of dislocations. Thus, the output power of 380 nm UV InGaN LEDs can be increased by reducing the number of dislocations using ELOG. Figure 10 shows the wavelength dependence of the external quantum efficiency in the GaN-based LEDs grown on sapphire substrates. In the shorter-wavelength range, the external quantum efficiency becomes lower with decreasing wavelength. This result is consistent with the above. On the other hand, the external quantum efficiency becomes higher with increasing wavelength. As regards the reason for this, it is thought that the crystal quality of the InGaN active layer of LEDs becomes poor when the indium mole fraction is increased. In figure 10, the highest external quantum efficiency is observed with wavelengths of 400 nm to 470 nm. It is interesting to consider how much the external quantum efficiency will be improved in the future. To do this, the temperature dependence of the output power was measured in order to estimate the internal quantum efficiency. Figure 11 shows the temperature dependence of the output power of InGaN LEDs with an emission peak wavelength of 400 nm.

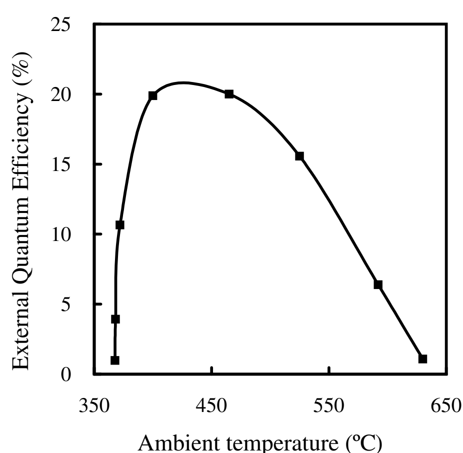

Figure 10. The wavelength dependence of the external quantum efficiency in the GaN-based LEDs grown on sapphire substrates.

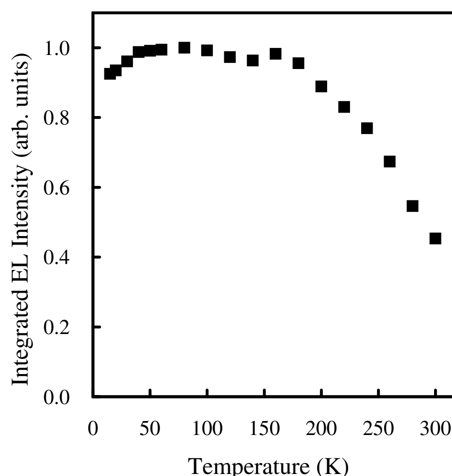

Figure 11. The temperature dependence of the output power of InGaN LEDs with an emission peak wavelength of 400 nm.

Taking the level between 50 °C and 150 °C to have the internal quantum efficiency of 100%, the internal quantum efficiency is about 50% at RT. This means that there is a possibility that the luminous efficiency will be improved remarkably by reducing the content of crystal defects such as point defects in the future.

6. Conclusions

GaN-based semiconductors have emerged as the leading materials for fabricating high-efficiency and high-reliability short-wavelength emitters. High-quality InGaN/GaN heterostructure UV/blue/green/amber LEDs were described. For general lighting use, much further improvement of luminous efficiency of LEDs is required, because the present luminous efficiency is not enough compared with that of fluorescent light. Therefore, it is very desirable to achieve an understanding of the intrinsic nature of GaN-based semiconductors and to control the crystalline quality.

Acknowledgments

We are grateful to the following collaborators who have made major contributions to this work: D Morita, H Narimatsu, M Yamada, K Takekawa and Y Narukawa.

References

[1] Amano H, Sawaki N, Akasaki I and Toyoda Y 1986 *Appl. Phys. Lett.* **48** 353
[2] Nakamura S, Mukai T and Senoh M 1992 *Appl. Phys.* **71** 5543
[3] Amano H, Kito M, Hiramatsu K and Akasaki I 1989 *Japan. J. Appl. Phys.* **28** L2112
[4] Nakamura S, Iwasa N, Senoh M and Mukai T 1992 *Japan. J. Appl. Phys.* **31** 1258
[5] Lester S D, Ponce F A, Craford M G and Steigerwald D A 1995 *Appl. Phys. Lett.* **66** 1249
[6] Chichibu S, Azuhata T, Sota T and Nakamura S 1996 *Appl. Phys. Lett.* **69** 4148
[7] Usui A, Sunakawa H, Sakai A and Yamaguchi A 1997 *Japan. J. Appl. Phys.* **36** L899
[8] Nam O H, Bremser M D, Zheleva T and Davis R F 1997 *Appl. Phys. Lett.* **71** 2638
[9] Nakamura S, Senoh M, Nagahama S, Iwasa N, Yamada T, Matsushita T, Kiyoku H, Sugimoto Y, Kozaki T, Umemoto H, Sano M and Chocho K 1998 *Japan. J. Appl. Phys.* **37** L309
[10] Nakamura S 1991 *Japan. J. Appl. Phys.* **30** 1620
[11] Nakamura S, Harada Y and Senoh M 1991 *Appl. Phys. Lett.* **58** 2021
[12] Nakamura S, Senoh M, Iwasa N and Nagahama S 1995 *Japan. J. Appl. Phys.* **34** L797
[13] Nakamura S, Senoh M, Iwasa N, Nagahama S, Yamada T and Mukai T 1995 *Japan. J. Appl. Phys.* **34** L1332
[14] Mukai T, Narimatsu H and Nakamura S 1998 *Japan. J. Appl. Phys.* **37** L479
[15] Mukai T, Morita D and Nakamura S 1998 *J. Cryst. Growth* **189+190** 778
[16] Kish F A and Fletcher R M 1997 *AlInGaP Light-Emitting Diodes* vol 48 (San Diego, CA: Academic) p 149
[17] Nakamura S 1998 *Science* **281** 956
[18] Chichibu S, Marchand H, Minsky M S, Keller S, Fini P T, Ibbetson J P, Fleischer S B, Speck J S, Bowers J E, Hu E, Mishra U K, DenBaars S P, Deguchi T, Sota T and Nakamura S 1999 *Appl. Phys. Lett.* **74** 1460